



DOI:10.22144/ctujoisd.2025.003

## Simulation of flow velocity variations in the Cai Khe Channel during sluice gate operation

Dinh Van Duy<sup>1\*</sup> and Nguyen Hoang Phuc<sup>2</sup>

<sup>1</sup>Faculty of Water Resource Engineering, College of Engineering, Can Tho University, Viet Nam

<sup>2</sup>Master student, Faculty of Water Resource Engineering, College of Engineering, Can Tho University, Viet Nam

\*Corresponding author (dvduy@ctu.edu.vn)

### Article info.

Received 23 Jul 2024  
Revised 29 Aug 2024  
Accepted 11 Feb 2025

### Keywords

Cai Khe barrier, Can Tho, flow velocity, flow-3D, MIDAS-ECM

### ABSTRACT

The three-dimensional hydraulic model Flow-3D was used to simulate the flow velocity in the Cai Khe channel when operating the gates of the Cai Khe barrier. Primary and secondary data were collected to build, calibrate, and validate the model. The NSE coefficient for calibration and validation cases were 0.74 and 0.61, respectively, indicating the reliability of the model. The case of operating the gate to discharge pollutants and create a unidirectional flow with a water level difference between the field and the river of 1.54 meters was chosen to check for potential erosion. The simulation results showed that at profiles 1 and 2 (located 10 meters and 60 meters from the center of the sluice towards the river, respectively), the average flow velocities were 2.97 m/s and 4.99 m/s, respectively, which are greater than the allowable non-erosive velocity ( $v_x = 0.19 - 0.26$  m/s). Therefore, the riverbed needs to be reinforced to prevent erosion when operating the sluice gates.

### 1. INTRODUCTION

Can Tho City, the center of the Mekong Delta region, is a prominent point on the economic and cultural map of Vietnam. With its strategic location on the main transportation axis of the western region, Can Tho city is not only an economic hub but also a center of culture, education, and science and technology in the area. The city's economy has grown robustly, with per capita gross domestic product higher than the national average, reflecting significant economic development and living standards. The development of Can Tho city extends beyond the economy to social sectors such as healthcare, education, and infrastructure, with the goal of continuously improving the quality of life for its residents. Additionally, the city plays an important role in national defense and security, thereby affirming its strategic position in the region

and the nation (Chinh et al., 2017; Minh Hoa & Khanh Linh, 2020).

However, climate change is significantly impacting Can Tho City. The main challenges the city faces include the risk of urban flooding due to rapid urbanization and changes in hydrometeorological conditions. The increase in impermeable surfaces and subsidence caused by groundwater extraction raise the flood risk in urban areas (Huong & Pathirana, 2013). Additionally, rising sea levels combined with increased river flow due to climate change are expected to heighten the risk of severe flooding in Can Tho city. Forecast models indicate that, under a scenario of unchanged urban development and rising sea levels, the city may endure worse flood events in the future (Huong et al., 2012; Huong & Pathirana, 2013; Chinh et al.,

2017; Minh Hoa & Khanh Linh, 2020; Ho et al., 2022).

Can Tho City, Vietnam, is actively addressing the challenges of climate change through various projects and initiatives aimed at reducing the city's vulnerability to extreme weather events and environmental impacts. The city has improved infrastructure to cope with droughts, salinity intrusion, and floods, including dredging canals, upgrading dikes, and constructing tidal control structures (Huong & Pathirana, 2013). However, operating the sluice gate can significantly affect river flow, potentially causing riverbank erosion. When the sluice gate is opened or closed, it can abruptly change the flow velocity in the river. This change can increase or decrease the water pressure on the riverbanks, leading to soil erosion and the displacement of materials along the river (Zuo et al., 2015; Vietz et al., 2018).

Therefore, this study was conducted to assess the impact of operating the sluice gate on changes in river flow velocity using a three-dimensional hydraulic model called FLOW-3D. The chosen study area is the Cai Khe sluice gate located on the Cai Khe channel in Ninh Kieu district, Can Tho City (Figure 1).

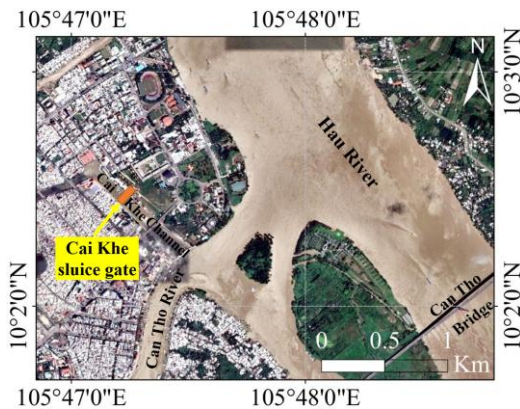


Figure 1. The study area



Figure 2. 3D view of the Cai Khe sluice gate (Cuong, 2020)

2. MATERIALS AND METHOD

The research steps are carried out as shown in the diagram in Figure 3. First, secondary data on the channel bed topography and sluice gate drawings were collected from the Cai Khe sluice gate design documents and used to build a 3D model. Simultaneously, primary data on flow velocity and water column height was measured and collected directly using the MIDAS-ECM, Levellogger Edge, and Hondex PS-7 handheld depth meter devices to simulate, calibrate, and validate the model. During the primary data collection process, sediment samples from the channel bed were also collected for particle size analysis to determine the non-erosive velocity of the channel.

Once calibrated and validated, the model is used to simulate the sluice gate operation scenarios to determine the flow velocity in the channel, compare it with the non-erosive velocity, and assess the potential for channel bed erosion when operating the sluice gate.

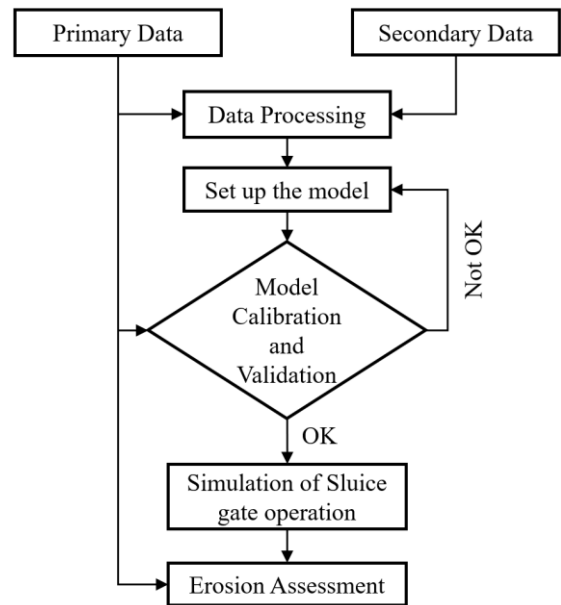
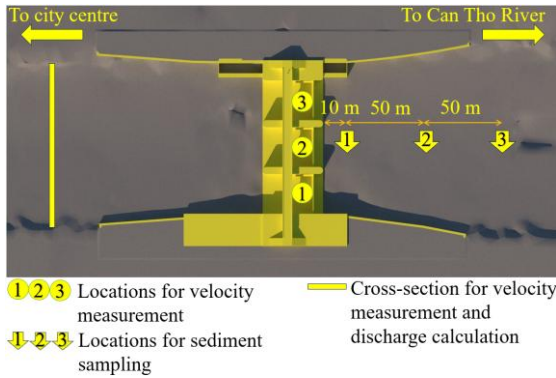


Figure 3. The research process

2.1. Primary data

Locations for flow velocity measurement and sediment sampling are shown in the plan view of the Cai Khe sluice gate shown in Figure 4. As illustrated, flow velocities were measured at locations 1, 2, and 3, which are situated in the middle of each gate opening. The measured velocities were used for the calibration and validation of the model. Meanwhile, sediment

samples were collected at distances of 10 m, 60 m, and 110 m from the center of the sluice gate towards the Can Tho River. The sediment samples were used to assess the potential for erosion caused by flow velocities during gate operation, which was modeled following the calibration and validation of the model.



**Figure 4. Locations for flow velocity measurement and sediment sampling**

2.1.1. Flow velocity measurement

Flow velocity was measured using the MIDAS-ECM device in combination with the automatic water level measurement device Levellogger Edge to synchronize the instantaneous velocity and depth data. Velocities were measured across the Cai Khe Barrier at locations 1, 2, and 3, as shown in Figure 4. These locations were chosen for the convenience of plotting the velocity profiles, as the riverbed at these sites is a fixed bed.



**Figure 5. Using Midas-ECM and Levellogger Edge to measure flow velocity**

2.1.2. Sediment sampling

Bed sediments were collected at locations 10 m, 60 m, and 110 m from the center of the sluice gate towards the Can Tho River (Figure 4). At each location, one sediment sample was collected and stored in a plastic container. The samples were collected using Ekman grab (Figure 6) and analyzed at the Housing Management and Construction Inspection Center in Can Tho City (LAS-XD 790) using the dry sieving (Figure 7) and hydrometer method (Figure 8) according to TCVN 4198-2014 standards (MOST, 2014).

The dry sieving method is determined by the following formula:

$$p_i = \frac{m_i}{m_0} \times 100 \tag{1}$$

Where:  $m_0$ ,  $m_i$ ,  $p_i$  are the mass of the soil sample used for the test, measured in grams (g); the mass of the particle group on the  $i^{\text{th}}$  sieve, measured in grams (g); and the percentage content of the particle group on the  $i^{\text{th}}$  sieve, respectively.

$$m_0^* = \sum_{i=1}^n m_i + m_{<0.1} \tag{2}$$

Where:  $m_0^*$ ,  $m_i$ ,  $m_{<0.1}$  are the mass of the soil sample after analysis, measured in grams (g); the mass of the particle group on the  $i^{\text{th}}$  sieve, measured in grams (g); and the mass of the particles passing through the 0.1 mm sieve, measured in grams (g), respectively.



**Figure 6. Sediment sampling**



**Figure 7. Dry Sieving Test Procedure Sample**

The hydrometer method is determined by the following formula:

$$P_{TL} = \frac{\rho_s(\rho_0 - 1)}{\rho_0(\rho_s - 1)} \times \frac{R_A}{m} \times (100 - K) \quad (3)$$

Where:  $P_{TL}$  is the cumulative percent retained in each sieve (%);  $\rho_s$ ,  $\rho_0$ ,  $m$ ,  $K$ ,  $R_A$  are the bulk density of soil particles, measured in grams per cubic centimeter ( $\text{g/cm}^3$ ); the assumed specific gravity used for calibration on the hydrometer, taken as  $2.65 \text{ g/cm}^3$ ; the dry mass of the soil sample, measured in grams (g); the total percentage content of particle groups on sieves of  $0.5 \text{ mm}$  and above; and the corrected reading of hydrometer type A, respectively.

$$R_A = R'_A + m_A + n_A - C_A \quad (4)$$

Where:  $R'_A$ ,  $m_A$ ,  $n_A$ ,  $C_A$  are the reading of hydrometer type A; the temperature correction of the suspension at the time of taking the  $R'_A$  reading; the meniscus correction of the suspension on the scale of hydrometer type A; and the dispersing agent correction, corresponding to the experiment using hydrometer type A, respectively.

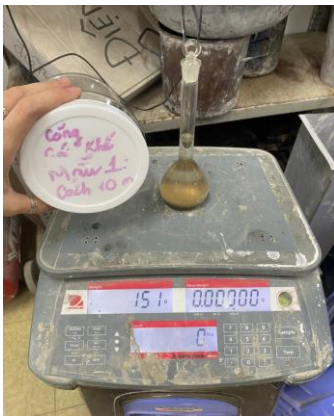


**Figure 8. Hydrometer testing method**

### 2.1.3. Determination of the allowable non-erosive velocity ( $V_{kx}$ )

The allowable non-erosive velocity is the maximum velocity that the flow can reach without causing erosion of the channel bed. The allowable non-erosive velocity is calculated according to (Kixelep, 2008) using formulas (5) and (6):

When the soil composition is homogeneous:

$$v_k = 1g \frac{8,8H}{d} \sqrt{\frac{2g(\gamma_1 - \gamma_n)d}{1,75\gamma_n}} \quad (5)$$

When the soil composition at the channel bed is heterogeneous:

$$v_k = \frac{2g(\gamma_1 - \gamma_n)d_{tb}}{1,75\gamma_n} 1g \frac{8,8H}{d_5} \quad (6)$$

Where  $v_k$  is the allowable non-erosive velocity (m/s),  $H$  is the water depth in the channel (m),  $d$  is the particle diameter (mm);  $d_5$  is the diameter of the largest particles that make up 5% of the total sediment volume (mm);  $d_{tb}$  is the average diameter of the sediment mixture (mm);  $\gamma_1$  and  $\gamma_n$  are the bulk densities of the sediment and water, respectively ( $\text{kN/m}^3$ ); and  $H$  is the flow depth (m).

## 2.2. Secondary data

Secondary data were collected from the ODA project management unit of Can Tho City. Detailed information on each type of data is presented in Table 1.

**Table 1. Secondary data**

| No. | Data             | Sources                                     |
|-----|------------------|---|
| 1   | Hydraulic report | ODA project management unit of Can Tho City |
| 2   | Bathymetric data | ODA project management unit of Can Tho City |
| 3   | Shop drawings    | ODA project management unit of Can Tho City |

## 2.3. Model setup, calibration, and validation

### 2.3.1. Model setup

Regarding the model geometry and meshing, the three-dimensional model of the Cai Khe sluice gate and channel bed was constructed based on the bottom topography data and the shop drawings of the Cai Khe sluice gate, as presented in Table 1. The three-dimensional image of the sluice gate and channel bed model after being input into the Flow-3D software is described in Figure 9. Concerning the meshing, a high-quality mesh is crucial for

numerical simulations. The computational mesh should achieve the desired accuracy while also reducing the number of simulations required. After conducting several simulation pre-checks, a cell size of 1 meter was chosen for the structured mesh along all axes. The simulation lasted for 10 minutes, with an initial time step set at 1 second. The time step was automatically adjusted during the simulation to maintain stability.

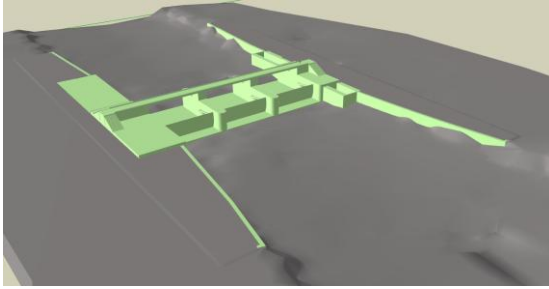


**Figure 9. 3D model of Cai Khe sluice gate**

Field-measured data, such as water level and flow velocity, were used for calculations and as boundary conditions for the model. Specifically, the flow rate data was assigned to the upstream boundary at the  $X_{min}$  cross-section, and the water column data was assigned to the downstream boundary at the  $X_{max}$  cross-section of the model.

**Table 2. Boundary conditions**

|           | $Q$ (m <sup>3</sup> /s) | $H$ (m) |             |
|-----------|-------------------------|---------|-------------|
| $X_{min}$ | 68.59                   |         |             |
| $X_{max}$ |                         | $t = 0$ | $t = 300$ s |
|           |                         | 4.4     | 4.055       |

2.3.2. Model calibration and validation

Simulations were conducted using FLOW-3D Hydro software. This software employs the discretization method to solve the partial differential equations of the Navier-Stokes and continuity equations. Equations (7) to (11) represent the Navier-Stokes and continuity equations, respectively.

$$\frac{\partial p}{\partial t} + \frac{\partial}{\partial x_i}(\rho u_i) = 0 \tag{7}$$

$$V_F \frac{\partial p}{\partial t} + \frac{\partial}{\partial x}(\rho u A_x) + R \frac{\partial}{\partial y}(\rho v A_y) + \frac{\partial}{\partial z}(\rho w A_z) = R_{DIF} + R_{SOR} \tag{8}$$

$$\frac{\partial u}{\partial t} + \frac{1}{V_F} \left\{ u A_x \frac{\partial u}{\partial x} + v A_y R \frac{\partial u}{\partial y} + w A_z \frac{\partial u}{\partial z} \right\} = -\frac{1}{\rho} \frac{\partial p}{\partial x} + G_x + f_x \tag{9}$$

$$\frac{\partial v}{\partial t} + \frac{1}{V_F} \left\{ u A_x \frac{\partial v}{\partial x} + v A_y R \frac{\partial v}{\partial y} + w A_z \frac{\partial v}{\partial z} \right\} = -\frac{1}{\rho} \left( R \frac{\partial p}{\partial y} \right) + G_y + f_y \tag{10}$$

$$\frac{\partial w}{\partial t} + \frac{1}{V_F} \left\{ u A_x \frac{\partial w}{\partial x} + v A_y R \frac{\partial w}{\partial y} + w A_z \frac{\partial w}{\partial z} \right\} = -\frac{1}{\rho} \frac{\partial p}{\partial z} + G_z + f_z \tag{11}$$

Where  $(u, v, w)$  are velocity components,  $(A_x, A_y, A_z)$  are fraction of flow-related area,  $(G_x, G_y, G_z)$  are body accelerations,  $(f_x, f_y, f_z)$  are viscosity accelerations in the directions  $(x, y, z)$ , the  $RSOR$  is the mass source; the  $RDIF$  is the turbulence expression; the  $VF$  is the volume fraction of the fluid, and the  $P$  represents the pressure (Daneshfaraz et al., 2016; Habibi et al., 2023).

The roughness coefficient, which is related to the shear stress, was used to calibrate the model. The calibration and validation of the model were also based on the accuracy analysis of flow velocity parameters using the Nash-Sutcliffe Efficiency (NSE) coefficient (Nash & Sutcliffe, 1970). The closer the NSE coefficient is to 1, the more accurate and reliable the simulation results.

$$NSE = 1 - \frac{\sum_{i=1}^n (V_{id} - V_{mp})^2}{\sum_{i=1}^n (V_{id} - \bar{V}_{id})^2} \tag{12}$$

Where  $V_{id}$ ,  $V_{mp}$ ,  $\bar{V}_{id}$  are measured velocity, simulated velocity, and mean measured velocity, respectively;  $n = 5$ .

**2.4. Simulation of Sluice Gate Operation**

The scenario of operating the sluice gate to discharge pollutants and create a one-way flow involves operating the gate with a water level difference of 1.94 meters between the fields and the river (0.40 meters in the fields and -1.54 meters in the river). This scenario was chosen for simulating gate operation because it is the operation case with the highest frequency of use (Cuong, 2020).

### 3. RESULTS AND DISCUSSION

#### 3.1. Field-measured velocity at three gate openings

The measured flow velocity at the three sluice gates is described in Figure 10. It can be observed that the maximum flow velocity at the three sluice gates is very similar, fluctuating around 0.3 m/s. However, the vertical distribution of the velocity differs significantly. This difference may be due to the varying bottom topography at the three sluice gate sections.

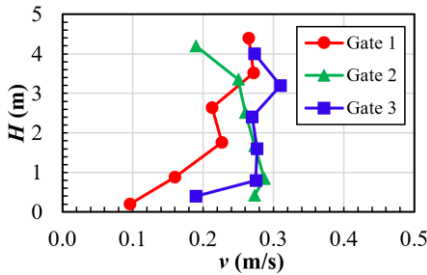


Figure 10. Measured flow velocity at the three gate openings

#### 3.2. Sediment grain size analysis

The particle-size distribution curve of the sediment sample at location 2 is shown in Figure 11. From this figure, the median particle diameter ( $D_{50}$ ), which is the diameter at which 50% of the soil mass is finer than this size (Pholkern et al., 2015), can be determined to be 0.04 mm. This value of  $D_{50}$  will be used later to determine the allowable non-erosive velocity of the bed material in the Cai Khe channel.

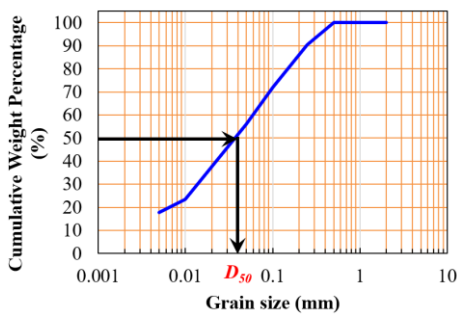


Figure 11. Particle-size distribution curve of sediment sample No.2

#### 3.3. Model calibration and validation

The simulated velocity at gate 1 is plotted against the measured velocity in Figure 12. It should be noted that this simulated velocity is based on the model without calibration. In this case, the Manning coefficients for the sluice gates and the channel bed

were chosen as 0.011 and 0.025, respectively (Akan & Iyer, 2021). The Nash-Sutcliffe Efficiency (NSE) was calculated and is shown in Table 3. As can be seen from the table, the NSE in this case is -0.41, indicating a significant difference between the observed and simulated velocities. Hence, the model must be calibrated.

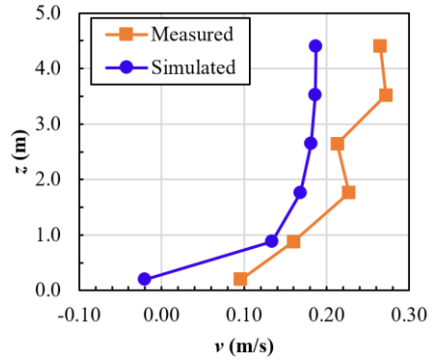


Figure 12. Measured and simulated velocity profiles at gate 1 before calibration

Table 3. NSE before calibration

| $z$ (m) | $v_{measured}$ (m/s) | $v_{simulated}$ (m/s) | NSE   |
|---------|----------------------|-----------------------|-------|
| 0.20    | 0.10                 | -0.02                 | -0.41 |
| 0.88    | 0.16                 | 0.13                  |       |
| 1.76    | 0.23                 | 0.17                  |       |
| 2.64    | 0.21                 | 0.18                  |       |
| 3.52    | 0.27                 | 0.19                  |       |
| 4.40    | 0.27                 | 0.19                  |       |

The velocity profile extracted from the model after three calibrations is shown in Figure 13. The corresponding NSE is also shown in Table 4. As illustrated in Figure 13, there is a good agreement between the measured and simulated velocities. The NSE value of 0.74 in Table 4 indicates the reliability of the calibrated model. The calibrated Manning coefficients for the sluice gate and the channel bed were 0.015 and 0.03, respectively.

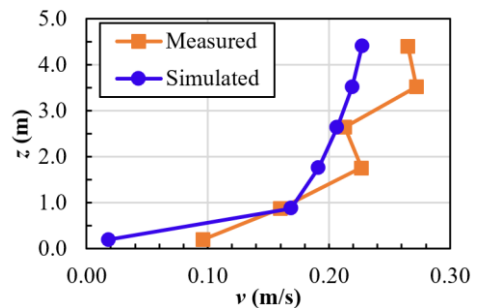
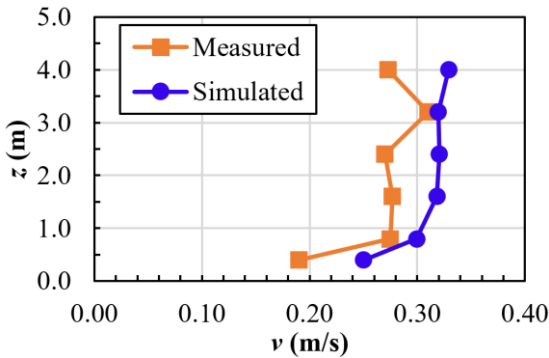


Figure 13. Measured and simulated velocity profiles at gate 1 after calibration

**Table 4. NSE after calibration**

| $z$ (m) | $v_{measured}$ (m/s) | $v_{simulated}$ (m/s) | NSE  |
|---------|----------------------|-----------------------|------|
| 0.20    | 0.10                 | 0.04                  | 0.74 |
| 0.88    | 0.16                 | 0.20                  |      |
| 1.76    | 0.23                 | 0.22                  |      |
| 2.64    | 0.21                 | 0.24                  |      |
| 3.52    | 0.27                 | 0.25                  |      |
| 4.40    | 0.27                 | 0.25                  |      |

After calibration, the model needs to be validated to ensure its stability and to detect any errors (if any) so that the model can be recalibrated. In this study's model validation process, the set of actual measured and simulated flow velocities at gate 3 of the Cai Khe sluice gates was used. The results of the model validation are presented in Figure 14 and Table 5. Although there are differences between the measured and simulated velocities, the stability of the calibrated model is acceptable, as indicated by an NSE coefficient of 0.61.



**Figure 14. Measured and simulated velocity profiles at gate 3 for validation**

**Table 5. NSE in the validation**

| $z$ (m) | $v_{measured}$ (m/s) | $v_{simulated}$ (m/s) | NSE  |
|---------|----------------------|-----------------------|------|
| 0.4     | 0.19                 | 0.25                  | 0.61 |
| 0.8     | 0.28                 | 0.30                  |      |
| 1.6     | 0.28                 | 0.32                  |      |
| 2.4     | 0.27                 | 0.32                  |      |
| 3.2     | 0.31                 | 0.32                  |      |
| 4       | 0.27                 | 0.33                  |      |

**3.4. Flow velocity change due to gate operation and potential erosion of the channel bed**

The simulated results from the Flow-3D model for the scenario of gate operation with a water level difference (1.94 m) are presented in Figure 15 and Figure 16. It can be observed that the flow velocity at a position 60 meters from the center of the sluice

gate is higher than the flow velocity just past the gate (10 meters from the center of the sluice gates).

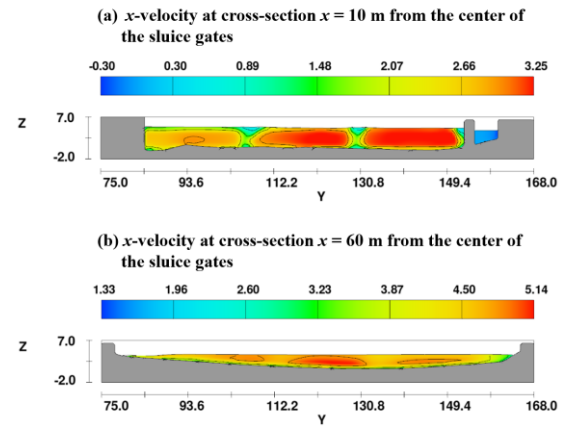


**Figure 15. Velocity distribution at cross-sections 10 m and 60 m from the center of the sluice gates**

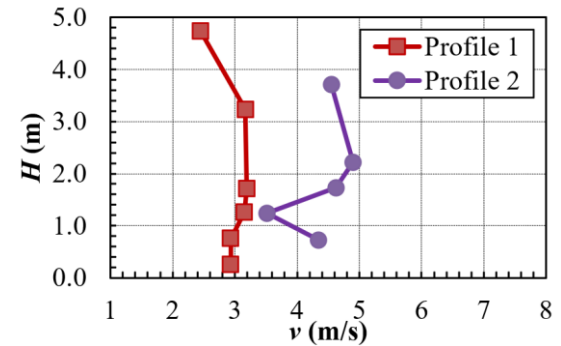


**Figure 16. Velocity profile at Cross-Section 1 (10 m from the sluice gate) and Cross-Section 2 (60 m from the sluice gate)**

Based on the sediment analysis results, the median particle diameter ( $D_{50}$ ) is 0.04 mm. According to the calculation of the allowable non-erosive velocity ( $v_k$ ) as per Vietnamese Standard TCVN 4118-2021 (TLU, 2021), for channels with an average depth ( $h_{tb}$ ) higher or equal to 3.0 m, the  $v_k$  ranges from 0.19 to 0.26 m/s. Meanwhile, the average velocities at cross-sections 1 and 2 are 2.97 m/s and 4.99 m/s, respectively, which are much higher than the non-erosive velocity ( $v_k$ ). Therefore, erosion will occur during sluice gate operation, and reinforcement measures are necessary.

**4. CONCLUSION**

The three-dimensional hydraulic model Flow-3D was used to simulate flow velocities in the Cai Khe channel during the operation of the Cai Khe sluice

gate. Primary and secondary data were collected to build, calibrate, and validate the model. The NSE coefficient for calibration and validation cases were 0.74 and 0.61, respectively, indicating the reliability of the model. The scenario of operating the sluice gate to discharge pollutants and create unidirectional flow with a water level difference of 1.94 m between the fields and the river was chosen to assess erosion. The simulation results show that at cross-sections 1 and 2 (10 m and 60 m from the sluice gate center, respectively), the average flow

velocities are 2.97 and 4.99 m/s, which are higher than the non-erosive velocity ( $v_k = 0.19 - 0.26$  m/s). Therefore, the riverbed needs to be reinforced to prevent erosion during sluice gate operation.

## 5. ACKNOWLEDGMENT

The authors sincerely thank Flow Science, Inc. for providing a free license of the Flow-3D (Hydro) software to the College of Engineering, Can Tho University.

## REFERENCES

- Akan, A. O., & Iyer, S. S. (2021). *Open channel hydraulics*. Butterworth-Heinemann.
- Chinh, D. T., Dung, N. V., Gain, A. K., & Kreibich, H. (2017). Flood Loss Models and Risk Analysis for Private Households in Can Tho City, Vietnam. *Water*, 9(5), 313. <https://www.mdpi.com/2073-4441/9/5/313>
- Cuong, P. H. (2020). *Report of construction design drawings* (Contract Package: TV3-CT17: Consulting for survey and design of Cai Khe-Hang Bang ship lock, Can Tho City).
- Daneshfaraz, R., Ghahramanzadeh, A., Ghaderi, A., Joudi, A. R., & Abraham, J. (2016). Investigation of the effect of edge shape on characteristics of flow under vertical gates. *Journal - American Water Works Association*, 108(8), E425-E432.
- Habibi, K., Fard, F. E., & Pari, S. A. A. (2023, 8-9 November 2023). Investigation of the flow field around bridge piers on a non-eroding bed using FLOW-3D. *22<sup>nd</sup> Iranian Conference on Hydraulics University of Maragheh, Maragheh, Iran*.
- Ho, B. Q., Nguyen, K. D., Vu, K. H. N., Nguyen, T. T., Nguyen, H. T. T., Ngo, D. D. N., Tran, H. T. H., Le, P. H., Nguyen, Q. H., Ngo, Q. X., Huynh, N. T. T., & Nguyen, H. D. (2022). Apply MIKE 11 model to study impacts of climate change on water resources and develop adaptation plan in the Mekong Delta, Vietnam: a case of Can Tho city. *Environmental Monitoring and Assessment*, 194(2), 765. <https://doi.org/10.1007/s10661-022-10185-7>
- Huong, H. T. L., Assela, P., & Thuc, T. (2012). Facing multiple challenges: the future of flooding in Can Tho city. *VNU Journal of Science: Earth and Environmental Sciences*, 28(2). <https://js.vnu.edu.vn/EES/article/view/1158>
- Huong, H. T. L., & Pathirana, A. (2013). Urbanization and climate change impacts on future urban flooding in Can Tho city, Vietnam. *Hydrol. Earth Syst. Sci.*, 17(1), 379-394. <https://doi.org/10.5194/hess-17-379-2013>
- Kixelep, P. G. A. A. D., Danhitsenko, N. V., Kaxpaxon, A. A., Griptsenko, G. I., Paskop, N. N., Xlixki, X. M. (2008). *Hydraulic Calculations Handbook*. Construction Publishing House.
- Minh Hoa, T. T., & Khanh Linh, C. (2020). Tourism and Environmental Security in Mekong Delta (Case Study in Can Tho City). *VNU Journal of Science: Policy and Management Studies*, 36(4). <https://doi.org/10.25073/2588-1116/vnupam.4273>
- MOST. (2014). *TCVN 4198:2014 Soils – Laboratory methods for particle - size analysis*.
- Nash, J. E., & Sutcliffe, J. V. (1970). River flow forecasting through conceptual models part I — A discussion of principles. *Journal of Hydrology*, 10(3), 282-290. [https://doi.org/https://doi.org/10.1016/0022-1694\(70\)90255-6](https://doi.org/https://doi.org/10.1016/0022-1694(70)90255-6)
- Pholkern, K., Srisuk, K., Grischek, T., Soares, M., Schäfer, S., Archwichai, L., Saraphirom, P., Pavelic, P., & Wirojanagud, W. (2015). Riverbed clogging experiments at potential river bank filtration sites along the Ping River, Chiang Mai, Thailand. *Environmental Earth Sciences*, 73(12), 7699-7709. <https://doi.org/10.1007/s12665-015-4160-x>
- TLU. (2021). *TCVN 4118 : 2021 Hydraulic structures – Water conveyance system – Requirements for design*.
- Vietz, G. J., Lintern, A., Webb, J. A., & Straccione, D. (2018). River Bank Erosion and the Influence of Environmental Flow Management. *Environmental Management*, 61(3), 454-468. <https://doi.org/10.1007/s00267-017-0857-9>
- Zuo, Q., Chen, H., Dou, M., Zhang, Y., & Li, D. (2015). Experimental analysis of the impact of sluice regulation on water quality in the highly polluted Huai River Basin, China. *Environmental Monitoring and Assessment*, 187(7), 450. <https://doi.org/10.1007/s10661-015-4642-z>